Investigation of factors that affect post-fire recovery of photosynthetic activity at global scale

Ecological Indicators 171 (2025) 113206

Contents lists available at ScienceDirect

Ecological Indicators

journal homepage: www.elsevier.com/locate/ecolind

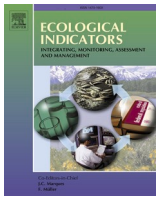

Original Articles

Investigation of factors that affect post-fire recovery of photosynthetic activity at global scale

Yicheng Shen [a,b,*], I. Colin Prentice [b,c], Sandy P. Harrison [a,b]

[a] Geography and Environmental Science, University of Reading, Whiteknights, Reading RG6 6AH United Kingdom
[b] Leverhulme Centre for Wildfires, Environment and Society, Imperial College London, South Kensington, London SW7 2BW United Kingdom
[c] Georgina Mace Centre for the Living Planet, Department of Life Sciences, Imperial College London, Silwood Park Campus, Buckhurst Road, Ascot SL5 7PY United Kingdom

ARTICLE INFO

Keywords:
Post-fire recovery
Photosynthetic activity
SIF
Vegetation regeneration
Fire adaptations

ABSTRACT

The time taken for ecosystems to recover after wildfire affects the rate of carbon sequestration, and this in turn impacts land–atmosphere exchanges and hydrological processes. Factors affecting post-fire recovery time have been investigated at site or regional scale, but there is comparatively little information about this at a global scale. In this study, we use solar-induced chlorophyll fluorescence (SIF) to estimate the recovery of photosynthetic activity after fire for more than 10,000 fires representing the range of ecosystems across the globe. We then examined the factors that influence post-fire recovery time, initially using the relaxed lasso technique to identify the most important factors and then using a linear regression model incorporating these factors. We show that vegetation characteristics, the characteristics of the fire, and post-fire climate all influence recovery time. Gross primary production (GPP) is the most important factor, with faster recovery in ecosystems with higher GPP. Fire properties which indicate substantial vegetation damage, such as fire intensity and duration, result in longer recovery times. Post-fire climate also affects recovery time: anomalous temperature and temperature seasonality, and higher than normal dry days increase recovery time while higher-than-average precipitation decreases recovery time. There is an additional impact of vegetation type (biome), which may reflect differences in plant adaptations to fire between biomes. We show that there is a clear relationship between the proportion of plants that resprout after fire in a biome and recovery time, with ecosystems characterised by higher abundance recovering faster.

1. Introduction

Fire is a widespread natural disturbance, playing an important role in shaping the ecosystems through reducing vegetation cover and continuity, initiating succession and changing vegetation composition (Bond et al., 2005; Harrison et al., 2010; Pausas and Keeley, 2009). The time taken for vegetation to recover after a fire influences the rate of carbon sequestration and hence impacts the terrestrial carbon cycle. The recovery process affects carbon storage and turnover times, which in turn can impact hydrological processes and land–atmosphere interactions through feedbacks involving changes in vegetation, CO_2 levels, and climate (Fan et al., 2023; Li and Lawrence, 2017; Marcos et al., 2023). Identifying the factors that influence recovery time after wildfire will improve our understanding of ecosystem resilience (González-De Vega et al., 2016; Marcos et al., 2023) and aid in developing land management to promote the sustainability of ecosystems (Francos et al., 2016; Ireland and Petropoulos, 2015; Jucker Riva et al., 2016).

Post-fire recovery times are known to vary considerably. Fire properties, such as the intensity of the fire, have been shown to have a significant negative relationship with regeneration ability in Spain (Díaz-Delgado et al., 2003). Higher fire severity, as measured by the delta Normalized Burn Ratio (dNBR) or Composite Burn Index (CBI), has been shown to lead to slower recovery because it results in more complete vegetation destruction such that the ecosystem must recover from an early successional stage (González-De Vega et al., 2016; Liu, 2016; Viana-Soto et al., 2017). Extreme high-intensity fires can trigger vegetation shifts, altering species composition and ecosystem structure (Keeley, 2009; Kruger, 1984; Smit et al., 2010). Factors such as fire size and heterogeneity in the severity of the fire have also been shown to affect post-fire recovery time. Turner et al. (1997), for example, showed

* Corresponding author.
E-mail address: yicheng.shen@pgr.reading.ac.uk (Y. Shen).

https://doi.org/10.1016/j.ecolind.2025.113206
Received 25 September 2024; Received in revised form 25 January 2025; Accepted 5 February 2025
Available online 11 February 2025

that recovery, both in terms of vegetation cover and species richness, was quicker after smaller fires than larger fires. Burnt patch perimeter-area ratio (PAR), the shape complexity that reflects the heterogeneity of burn severity, has also been shown to affect recovery time: higher heterogeneity is more likely to enhance post-fire vegetation regeneration since less severely burned or unburned 'islands' can act as seed sources (João et al., 2018). Topographic factors such as aspect has been shown to influence recovery, Ireland and Petropoulos (2015), for example, showed that regeneration was faster on north-facing slopes than to south-facing slopes in western Canada while Shryock et al. (2015) found that vegetation recovery in the Sonoran Desert was faster at higher elevation sites. The long-term climate has also been shown to be important for recovery. Giorgis et al. (2021) showed that ecosystems characterised by higher temperatures and water availability recovered more quickly after fire by comparing several studies from South America. Shryock et al. (2015) found that vegetation recovery after fire in the Sonoran Desert was fastest in areas with higher average annual precipitation. The climate after the fire has also been shown to affect recovery time: higher than normal precipitation in the year after fire has a positive influence on postfire recovery (Liu, 2016; Meng et al., 2015). Little work has been done to quantify the impact of vegetation properties which might affect fuel loads and continuity, such as gross primary production (GPP), on recovery time. Other ecosystem properties, such as plant adaptations to fire such as resprouting, serotiny or heat- or smoke-induced germination, are known to influence the rate of post-fire recovery (Clarke et al., 2010; Clarke et al., 2013; Harrison et al., 2021; Lawes and Clarke, 2011). Serotiny, for example, allows seeds to be released in place without the need for migration of propagules from outside the fire-affected area, while resprouting produces even faster recovery through rapid regeneration from meristems. However, again there has been little work to quantify this.

Remote-sensing data has been used to investigate vegetation recovery after specific fire events by comparing the remote sensed vegetation parameters before and after a fire (Gitas et al., 2012; Viana-Soto et al., 2022; Zhou et al., 2019). The most frequently used data are optical remote sensing products from sensors such as the Moderate Resolution Imaging Spectroradiometer (MODIS), the Advanced Very High Resolution Radiometer (AVHRR) and Landsat. For example, Liu (2016) showed that the shortwave infrared (SWIR) vegetation index from Landsat could be used to quantify post-fire recovery in boreal larch forests. The recent development of products from microwave and LiDAR (Light Detection And Ranging) remote sensing sensors has been used to examine biomass recovery in dense forests after fire. Zhou et al. (2019) and De Luca et al. (2022) monitored the post-fire vegetation regrowth through c-band SAR backscatter data. Bousquet et al. (2022) compared the performance of different vegetation optical depth (VOD) bands and showed that L-VOD can be used to monitor post-fire recovery, especially over densely vegetated areas. Sato et al. (2016) quantified post-fire changes in forest canopy height and biomass using an airborne LiDAR sensor in western Amazonia, and LiDAR and multispectral data have been combined to assess post-fire forest structure recovery after fire in Mediterranean pine forests (Viana-Soto et al., 2022). Remote sensing products from microwave and LiDAR sensors, however, are only available for a limited time period, limiting their usefulness in ecosystems that recover slowly. However, the use of optical remote sensing products for investigating vegetation recovery is complicated by saturation of the signal such that vegetation "greenness" indexes reach a plateau although the vegetation biomass may continue to increase, leading to underestimates of recovery time in areas with high vegetation cover (Liu et al., 2012; Wang et al., 2019). Furthermore, surface properties and vegetation type affect light reflection and absorption, which can bias estimates of recovery time (Meroni et al., 2009; Mohammed et al., 2019). The nature of the bias is context specific: over dark surfaces, NDVI values are larger than would be expected for a given amount of vegetation than if the background is lighter, leading to an underestimate of recovery time, and the converse is true over very light surfaces such as dry, sandy soils.

Solar-induced chlorophyll fluorescence (SIF) distinguishes the energy emitted by plant chlorophyll after light absorption within the 600–800 nm wavelength range (Baker, 2008; Mohammed et al., 2019) and therefore provides a direct measure of photosynthetic activity at large spatial and temporal scales. It has also been considered a useful tool to monitor vegetation changes (Guo et al., 2020; Irteza et al., 2021; Mohammed et al., 2019; Zhang and Peñuelas, 2023). Qin et al. (2022) showed SIF was a reliable way of monitoring the loss and recovery of vegetation after both fire and drought. Guo et al. (2021) demonstrated that SIF reflects the recovery process after fire in boreal forests better than vegetation indices such as the Normalized Difference Vegetation Index (NDVI) or the Enhanced Vegetation Index (EVI). Xu et al. (2024) used SIF-based GPP investigated post-fire recovery time at the global scale and showed that it is more sensitive to the impact of fire disturbances than the kernel normalized difference vegetation index (kNDVI) or EVI.

In this study, we use SIF to estimate post-fire recovery time of photosynthetic activity for more than 10,000 individual fires worldwide. The recovery of photosynthetic activity is the necessary first step to full ecosystem recovery, expressed by recovery of biomass or ecosystem structure. Furthermore, although photosynthetic activity is only one aspect of post-fire recovery, SIF data are available at sufficient spatial and temporal resolution to characterise recovery after individual fires. We then investigate the fire, vegetation, climatic, topographic and human factors influencing the speed of post-fire recovery and how they operate, with the goal of determining how best to model post-fire recovery and thus improve our ability to capture the impact of fire disturbance on the carbon cycle.

2. Methods

2.1. Estimating post-fire recovery time for individual fires

The Fire Atlas (Andela and Jones, 2024; Andela et al., 2019) provides information on the location of ignitions, size and duration for individual fires that occurred between January 2002 to February 2024. We selected candidate fires that (a) were larger than the 0.05° grid cell resolution of the SIF data used as a measure of ecosystem state and (b) occurred in grid cells that had not been burnt in the previous three years and could therefore be assumed to be undisturbed. As a result of this selection criterion the fire candidates were taken from the interval after January 2005. We used land cover information provided in the Fire Atlas for each fire to remove fire candidates from grid cells classified as cropland, water, urban and built-up or where land cover was not specified.

We used SIF measurements of photosynthetic activity as an index of both the pre-fire and post-fire ecosystem state. The SIF data were derived from the Long-term spatially Contiguous Solar-Induced Fluorescence (LCSIF) product (Fang et al., 2023). LCSIF leveraged the red band and near-infrared band from MODIS and AVHRR to reproduce the Orbiting Carbon Observatory-2 (OCO-2) SIF using a neural network. The LCSIF product provides bi-weekly values covering the period between 1982 and 2022 at 0.05° resolution. We used the LCSIF data from 2002 onwards, corresponding to the start date of records from the Fire Atlas. We estimated monthly values of LCSIF as the largest of the two bi-weekly values in each month. We extracted the area weighted average value of LCSIF per month for each fire candidate. We used the maximum monthly value recorded in the three years preceding the fire to represent the vegetation state pre-fire. We used the maximum monthly value for each year after the fire to determine the trajectory of recovery (Fig. S1), where recovery was defined as 90 % of the pre-fire LCSIF value following Bastos et al. (2011). Alternative metrics, such as relative recovery within five years and recovery to 50 % of pre-fire SIF, were tested but found unsuitable for ecosystem-wide analysis (see Supplementary Section 3).

2.2. Data on potential factors affecting recovery time

We selected 28 variables that are thought to influence recovery time, categorized into five groups: fire characteristics, climate factors, vegetation factors, topographic factors, and human activity.

2.2.1. Fire characteristics

We used fire size, fire intensity, fire duration and fire speed as measures of fire properties that could influence recovery time, hypothesising that fire intensity, duration and rate of spread could affect the completeness of vegetation destruction while fire size could influence the speed of post-fire recolonisation of the burned area. Fire duration, fire size and fire speed data were obtained directly from the Fire Atlas. We also used the perimeter-area ratio (PAR), as a measure of the heterogeneity of burn severity in a fire (João et al., 2018), calculated by dividing the perimeter of the fire polygon by its area, where the fire perimeter and fire size data were taken from the Fire Atlas. Fire intensity was estimated by normalising fire radiative power (FRP), obtained from the MODIS MCD14ML dataset (Giglio et al., 2006), by the square root of fire size following Haas et al. (2022). We used pre-fire plant cover information, specifically tree cover, shrub cover, grass cover and bare ground, as measures of other vegetation properties that could affect fires, hypothesising that tree cover and shrub cover would reflect the likelihood of the occurrence of crown fires and hence be positively related to fire intensity while grass cover would reflect the likelihood of less intense surface fires. We included pre-fire bare ground as a measure of fuel continuity, which would also influence intensity and fire spread. We obtained plant cover from the Global Plant Functional Types (PFT) dataset (v2.0.8) at 300 m resolution (Harper et al., 2023). To calculate total tree cover, we aggregated the cover of all tree types within the dataset. Similarly, we derived the total shrub cover by combining the cover of all shrub types. Grass cover was determined using the cover of natural grasses, and bare cover was extracted directly. We converted the data to 0.05° via bilinear interpolation and extracted the percentage of the four land cover types one year before the fire using the area weighted average value for each fire candidate.

2.2.2. Climate factors

We used climatological data on annual mean temperature, temperature seasonality, total precipitation, precipitation seasonality, maximum dry day length, number of dry days, and number of frost days since these factors influence both ecosystem properties and fire occurrence (Haas et al., 2022; Harrison et al., 2010; Jennings and Harris, 2017). Climate data were obtained from the European Centre for Medium-Range Weather Forecasts (ECMWF) Reanalysis v5 (ERA5) dataset (Hersbach et al., 2023) and converted to 0.05° resolution via bilinear interpolation. Climatological values were derived by averaging data from 1990 to 2019 (30 years) and then calculating the area-weighted average for each fire candidate. Annual mean temperature was calculated as the average of daily mean temperature. Total precipitation was calculated as the sum of daily precipitation over the year. Precipitation and temperature seasonality were derived using the coefficient of variation, calculated by dividing the standard deviation by the mean of the daily total precipitation and daily temperature respectively for each year. Dry days were defined as days with less than 1 mm of precipitation, summed over the year to provide total number of dry days and summed over consecutive dry day intervals to determine the maximum dry day length. The number of frost days was calculated as the annual sum of days with temperature below 0 ℃. We then calculated how post-fire conditions deviated from this climatology to determine whether this influenced recovery rates, by calculating the difference between the average values obtained for the subsequent years after fire until recovery, and the long-term climatological values.

2.2.3. Vegetation factors

We used GPP to investigate the impact of vegetation productivity and its seasonality on post-fire recovery time. Monthly GPP data was obtained from the Breathing Earth System Simulator (BESS) v2.1 at 0.05° (Jeong et al., 2024; Li et al., 2023). Yearly total GPP was derived by summing the monthly GPP values and the yearly totals for the interval 1990–2019 were summed to produce a 30 years long-term average GPP. GPP seasonality was given by the coefficient of variation, calculated by dividing the standard deviation of the monthly GPP by the mean of the monthly GPP for each year. We then averaged yearly GPP seasonality over 30 years to obtain the long-term GPP seasonality. GPP and GPP seasonality were extracted using their area weighted average for each fire candidate.

2.2.4. Human activity

We used human population density as an index of the potential impact of fire or vegetation management practices on post-fire recovery time, hypothesising that, at a global scale, densely populated regions are generally more likely to be characterised by practices to minimise fire damage and promote post-fire restoration. Human population density was obtained from UN WPP-Adjusted Population Density, v4.11, part of the Gridded Population of the World (GPW) v4 (CIESIN, 2018). This dataset provides estimates of population density for the years 2000, 2005, 2010, 2015, and 2020, based on counts consistent with national censuses and population registers with respect to spatial distribution, but adjusted to match United Nations country totals. We applied linear interpolation to get the yearly population density from 2000 to 2020 and extracted the human population density for each fire candidate one year before the fire using the grid-cell area weighted average for each fire candidate.

2.2.5. Topographic factors

Topographic factors, such as elevation, aspect and slope, influence vegetation recovery by shaping the microclimate and soil conditions. Steep slopes at higher elevations, for example, are characterised by colder conditions and rapid runoff and vegetation recovery is likely to be slower under such conditions. Moisture retention also varies between north- and south-facing slopes, leading to differences in recovery rate between these locations. We used a “northness” index which combines information about both slope and aspect: in the Northern Hemisphere, a northness value close to 1 indicates a northern exposure on a vertical slope, while a value close to −1 indicates a vertical south-facing slope. To reflect differences in radiation receipts on north-facing slopes in the northern and southern hemisphere, we assigned negative values to northness in the northern hemisphere and positive values to northness in the southern hemisphere. We obtained northness and elevation from the GMTEDmd 5 km resolution topography data (Amatulli et al., 2018). We converted the resolution from 5 km to 0.05 degree by bilinear interpolation and extracted the northness and elevation using the area weighted average for each fire candidate.

We hypothesised that difference in the prevalence of adaptions to fire in different vegetation types could provide additional information about post-fire recovery time. We used the Hengl potential natural vegetation (PNV) map (Hengl, 2018; Hengl et al., 2018), which provides biome information at 250 m resolution. Each candidate fire was assigned to a biome based on the most frequently occurring biome within the fire polygon, provided it covered more than 50 % of the total area. Fire polygons characterised by multiple biomes and where no one biome occupied an area $>$ 50 % were not considered in this analysis.

2.3. Data analysis

We applied the relaxed lasso technique (Hastie et al., 2020) to these 28 factors to identify and rank important variables. Relaxed lasso is a variant of the lasso (Least Absolute Shrinkage and Selection Operator) regression used for both variable selection and regularization to enhance the prediction accuracy and interpretability of statistical models. Relaxed lasso produces sparser models than regular lasso but with equal

or lower prediction loss for high-dimensional data by including both soft- and hard-thresholding of estimators (Meinshausen, 2007) and has more interpretable coefficients (Hastie et al., 2020). We applied the relaxed lasso technique using the *glmnet* R package (Tay et al., 2023). Log or square-root transformations were applied to reduce the skewness of some variables and all variables were transformed to z-scores before applying relaxed lasso to ensure the coefficients were meaningful (Table 1).

The relaxed lasso helps with variable selection and improves prediction accuracy but there may still be collinearity between the selected variables. We therefore built a simple linear model after removing variables from the relaxed lasso analysis that were not significant or had variance inflation factors (VIFs) larger than 5 to avoid multicollinearity.

Finally, we included biomes as dummy variables in the simplified linear model to see whether this conferred additional explanatory power. We considered the 4323 fire candidates where the dominant biome covered > 50 % of the fire area of each fire candidate. We used Residual Standard Error (RSE), the Akaike information criterion (AIC) and the Bayesian information criterion (BIC) to evaluate the significance of including biomes in the model. We then examined recovery time across different biomes while controlling for other potentially confounding factors. To explore whether the biome encapsulates information about fire adaptations, we examined the relationship between post-fire recovery time and the abundance of resprouting plants, a trait chosen because there is more quantitative data on the abundance of resprouters within biomes compared to other fire-related traits. Plot-level species abundance data were derived from sPlotOpen (Bruelheide et al., 2019; Sabatini et al., 2021), which provides information on the relative cover of individual species derived by normalising the cover of all species to 1 in each plot. We calculated the relative cover of resprouters for each plot using species cover data and species resprouting information from Shen et al. (2023) in Europe and Australia. Only plots that recorded all vascular plant were considered. We then calculated the relationship between recovery time and the proportion of resprouters for each biome. Scatter plots were used to visualise this relationship and R^2 was used to evaluate how much variance in recovery time was explained by resprouting abundance.

3. Results

3.1. Post-fire photosynthetic recovery time

There were 19,432 fire candidates that met the screening requirements, but post-fire recovery time could only be measured for 10,026 (ca 52 %) of these fires either because they did not reach the 90 % threshold used to indicate recovery before the next fire occurred (5,967 fires) or because recovery was not achieved by the end of the sampling period (3,439 fires). Nevertheless, the remaining 10,026 fires are widespread across the globe and sample a range of vegetation types (Fig. 1A), although there are large numbers of fire candidates in northern Australia and parts of central Eurasia. Post-fire recovery times ranged from 1 year to 16 years (Fig. 1B), although in 75 % of the cases recovery occurred in < 4 years.

3.2. Factors influencing recovery time

The relaxed lasso identified 19 out of the 28 pre-selected potential factors as being important (Fig. 2, Table S1, Table S2). These factors include vegetation characteristics, fire properties and climate. None of the topographic or human activity factors were found to be important in this analysis.

The relaxed lasso identified GPP as the most important factor, with a negative relationship to recovery time such that ecosystems with higher GPP have shorter recovery times. GPP seasonality was also selected by relaxed lasso although it only had moderate importance. Temperature was the second most important factor from the relaxed lasso, with a negative relationship to recovery time. Temperature seasonality was also selected by the relaxed lasso although it only had moderate importance. The length of dry days was selected by the relaxed lasso, with longer dry periods leading to faster recovery. Precipitation seasonality was also selected, and showed a positive relationship with recovery time separately. Post-fire climate was also important for recovery time. Anomalously high temperature, increased temperature or precipitation seasonality, along with larger-than-normal number of frost days or larger-than-normal number of dry days increased recovery time while

Table 1
Information about the initial selection of predictor variables.

Variable	Variable details	Units	Transformation	Group
fire duration	Fire duration of the specific fire	day	square root	Fire
fire intensity	Fire intensity of the specific fire	megawatts km^{-1}	square root	Fire
fire size	Fire size of the specific fire	km^2	log	Fire
fire speed	Fire speed of the specific fire	km day^{-1}	log	Fire
PAR	Perimeter-area ratio	km^{-1}	log	Fire
tree cover	Percentage of tree cover	%		Fire
bare cover	Percentage of bare cover	%		Fire
grass cover	Percentage of grass cover	%		Fire
shrub cover	Percentage of shrub cover	%		Fire
temperature	Annual mean temperature	K	log	Climate
precipitation	Annual total precipitation	mm	square root	Climate
temperature seasonality	Coefficient of variation of temperature		log	Climate
precipitation seasonality	Coefficient of variation of precipitation			Climate
number of frost days	Number of frost days (temperature < 0 ℃)	day		Climate
number of dry days	Number of dry days (precipitation < 1 mm)	day	log	Climate
dry day length	Maximum length of consecutive dry days	day	log	Climate
Δ temperature	Anomalies of temperature	K		Climate
Δ precipitation	Anomalies of total precipitation	mm		Climate
Δ temperature seasonality	Anomalies of temperature seasonality			Climate
Δ precipitation seasonality	Anomalies of precipitation seasonality			Climate
Δ number of frost days	Anomalies of number of frost days (temperature < 0 ℃)	day		Climate
Δ number of dry days	Anomalies of number of dry days (precipitation < 1 mm)	day		Climate
Δ dry day length	Anomalies of maximum length of consecutive dry days	day		Climate
GPP	Gross primary production	gC m^{-2} d^{-1}	log	Vegetation
GPP seasonality	Coefficient of variation of gross primary production			Vegetation
elevation	Elevation	m		Topography
northness	Combines sun exposure and steepness of slope			Topography
population density	Population density	persons km^{-2}		Human activity

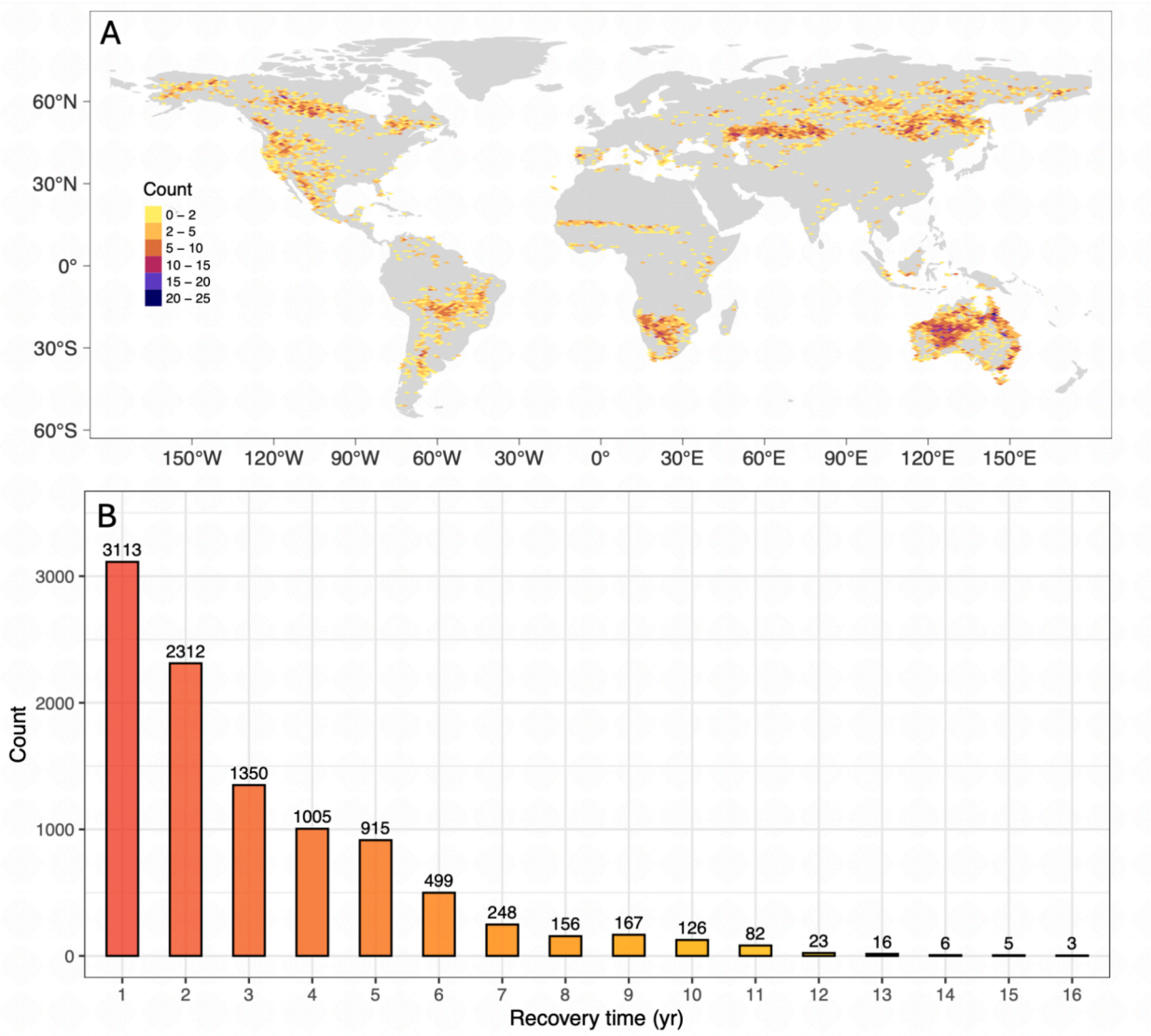

Fig. 1. (A) The geographic distribution of fire candidates used in this study, where the colour coding indicates the number of fires in the grid cell. (B) The distribution of post-fire recovery times for the fire candidates where recovery was complete during the sampling interval.

higher-than-average precipitation decreased recovery time.

All the fire-related properties were selected in the relaxed lasso, except for PAR and bare ground cover. Fire duration, fire intensity and fire speed were identified as highly important factors. Fire duration and fire intensity both showed positive relationships with post-fire recovery time, while fire speed showed a negative relationship. Tree cover and shrub cover were relatively important and have positive relationships with recovery time. Although fire size and grass cover were selected in the relaxed lasso, they both had an importance very close to zero.

Although factors related to human activity were not selected in the relaxed lasso, this may be due to the global scale of this analysis. Application of the relaxed lasso to fire candidates from a single biome, applied to biomes which had more than 500 samples, showed that human activity had relatively high importance in cold evergreen needleleaf forests (Table S3). However, it was not important in tropical savannas or steppes.

The linear regression model constructed using all of the factors identified as important by the relaxed lasso explained 39 % of the variability in post-fire recovery time. However, several of the factors identified as important by the relaxed lasso had VIFs larger than 5, indicating an unacceptable level of multicollinearity. These factors included temperature (VIF = 19.19), temperature seasonality (VIF = 11.89), GPP seasonality (VIF = 9.86), and precipitation seasonality (VIF = 6.32). Fire size, grass cover, shrub cover, anomalies of precipitation seasonality and anomalies of number of frost days were also excluded from the final model because of their insignificance in the linear regression (Table S5). The reduced model with only 11 explanatory factors explained 35 % of the variance in recovery time (Table 2, Fig. 3) which is only 4 % lower than the linear model including all 19 factors (Table S5). The direction of the relationships in the linear model (Fig. 3) was consistent with those in the relaxed lasso model, although the relative importance of some factors was changed. GPP was still the most important factor, followed by tree cover and fire duration. The negative relationship with GPP is consistent with faster recovery when the ecosystem is highly productive. The positive relationship with fire duration and with fire intensity, and the negative relationship with fire speed, are all consistent with the hypothesis that more time is needed to recover after severe fires. Tree cover and shrub cover both reflect the likelihood of crown fires, which are generally larger and more intense, and thus the positive relationship between these factors and recovery time is also consistent with more damage leading to longer recovery time. Dry day length showed a stronger negative relationship with post-fire recovery time than in the relaxed lasso. This somewhat counter-intuitive result probably reflects the fact that ecosystems in drier

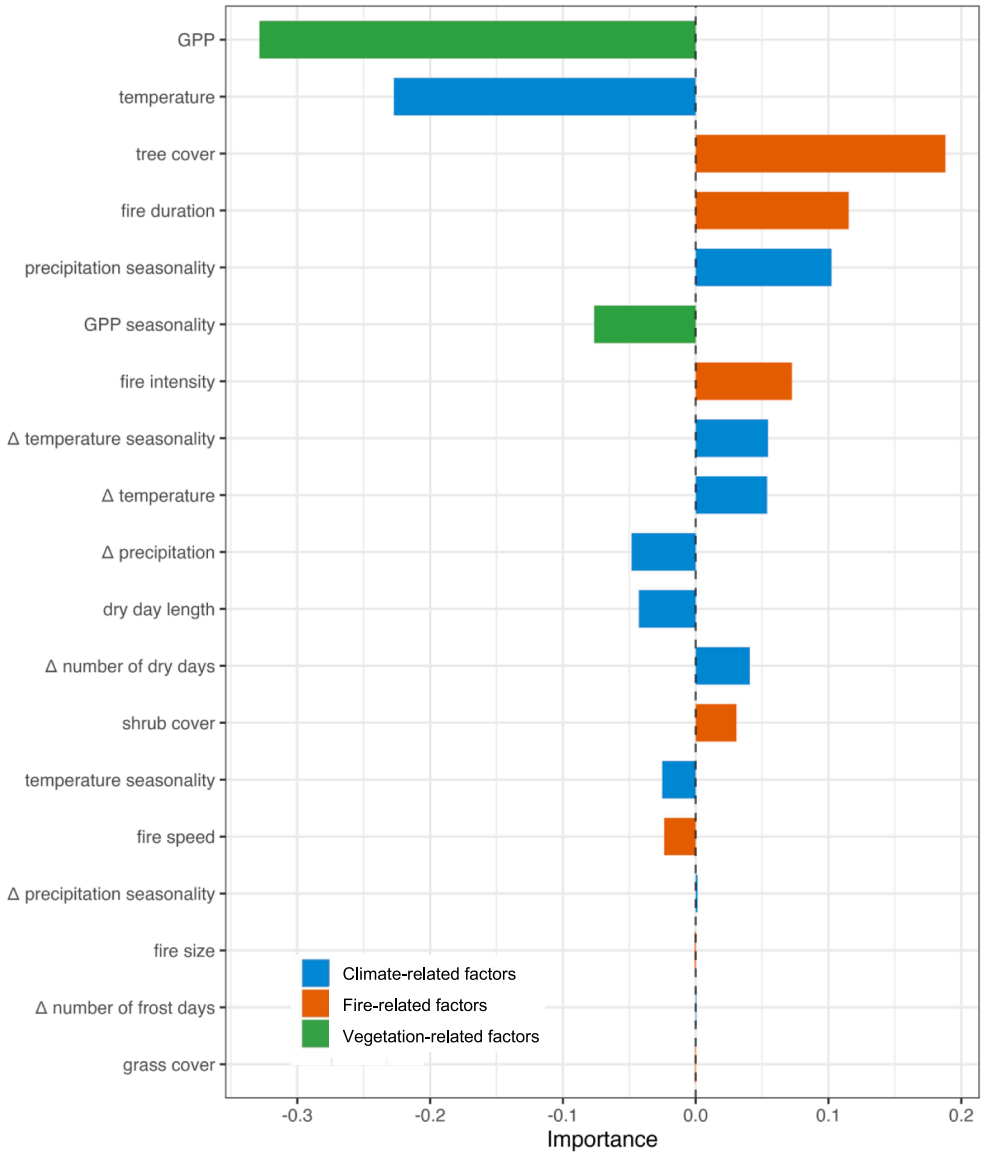

Fig. 2. Importance of factors impacting post-fire recovery of photosynthetic activity, where Importance is determined by the absolute values of the coefficients from the relaxed lasso model. For lasso model selection details, see Tables S1 and S2.

Table 2
Summary statistics of the final linear regression model. The order of factors follows the importance determined by the absolute t values. The Variance Inflation Factor (VIF) is a measure of the amount of multicollinearity. The significance codes (Pr(>|t|)) indicate the level of statistical significance: *** for p ≤ 0.001, ** for p ≤ 0.01.

	Estimate	Std. Error	t value	Pr(>|t|)	VIF
(Intercept)	0.88	0.01	148.94	***	
GPP	−0.42	0.01	−52.63	***	1.83
Tree cover	0.21	0.01	22.51	***	2.63
Fire duration	0.14	0.01	17.90	***	1.72
Fire intensity	0.09	0.01	14.14	***	1.14
Dry day length	−0.08	0.01	−10.43	***	1.77
Δ Temperature seasonality	0.08	0.01	10.25	***	1.70
Δ Temperature	0.08	0.01	9.59	***	1.78
Shrub cover	0.04	0.01	5.93	***	1.32
Δ Precipitation	−0.05	0.01	−5.29	***	2.54
Δ Number of dry days	0.03	0.01	2.98	**	2.74
Fire speed	−0.02	0.01	−2.98	**	1.24
				$R^2 = 0.35$	

conditions would experience more fires and thus are probably either dominated by grasses (Fig. S2) or dominated by species with adaptations to fire, such as resprouting, that promote rapid recovery (Fig. S3). Although less important than other factors, post-fire climate conditions still had an important influence on recovery time, with anomalously wet conditions (indicated by precipitation) leading to more rapid recovery and anomalously dry conditions (indicated by temperature, temperature seasonality, number of dry days) to less rapid recovery. See (Fig. 4).

3.3. The additional influence of biomes on recovery time

Including biome as a dummy variable in the linear model led to an increase in R^2 from 0.39 to 0.43 and a reduction in the RSE, AIC and BIC values (Table 3) indicating that vegetation type conveys additional information. Post-fire recovery time showed significant differences between biomes, after controlling for other variables by setting them to their median values. There is a gradual increase in recovery time moving from biomes characteristic of hot or dry or seasonally dry climates (e.g., tropical savanna, xerophytic woods/scrub) through forest biomes (e.g., warm-temperate evergreen broadleaf and mixed forest) to biomes

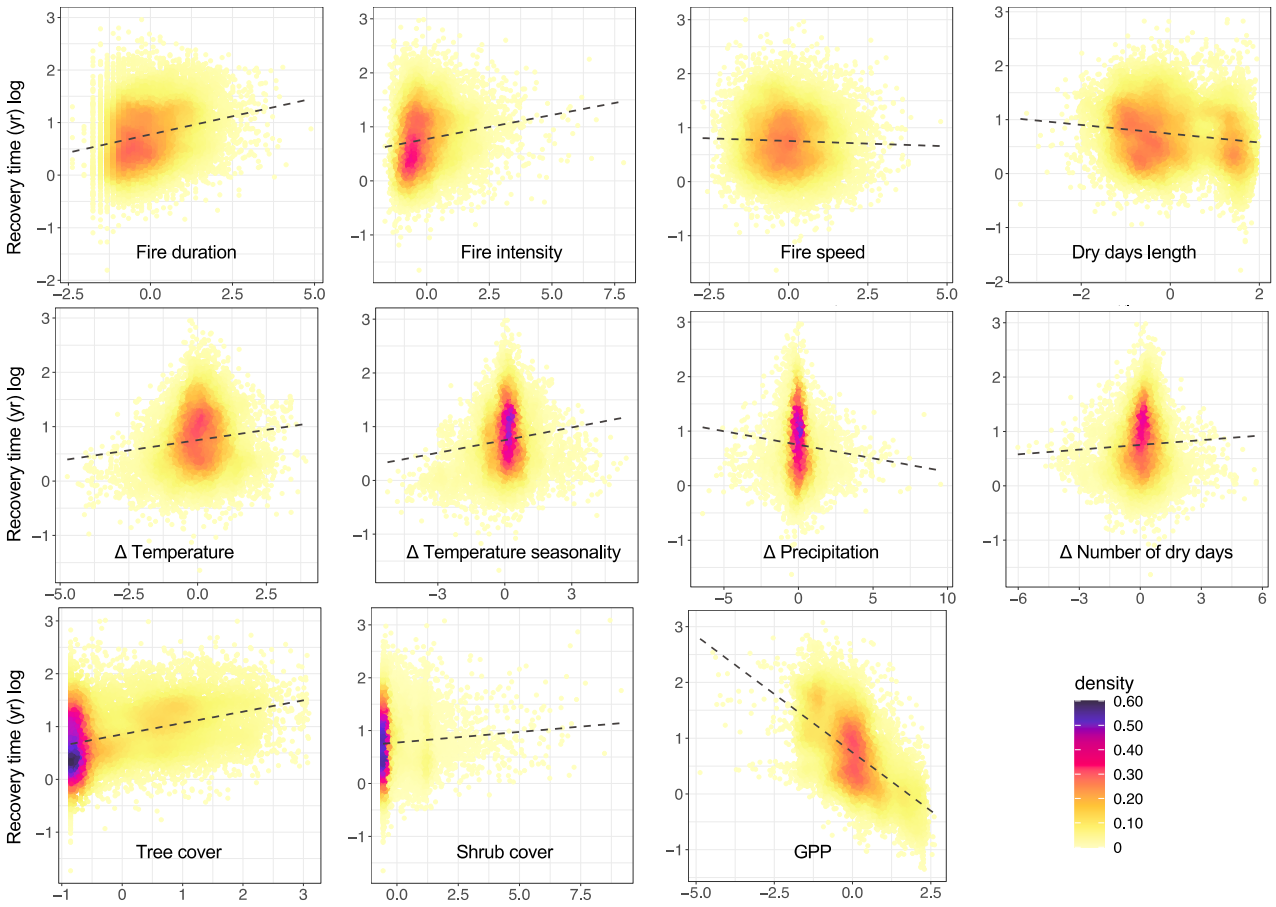

Fig. 3. Partial residual plots showing the relationship between recovery time and individual factors in the final linear regression, assuming that all other factors are constant.

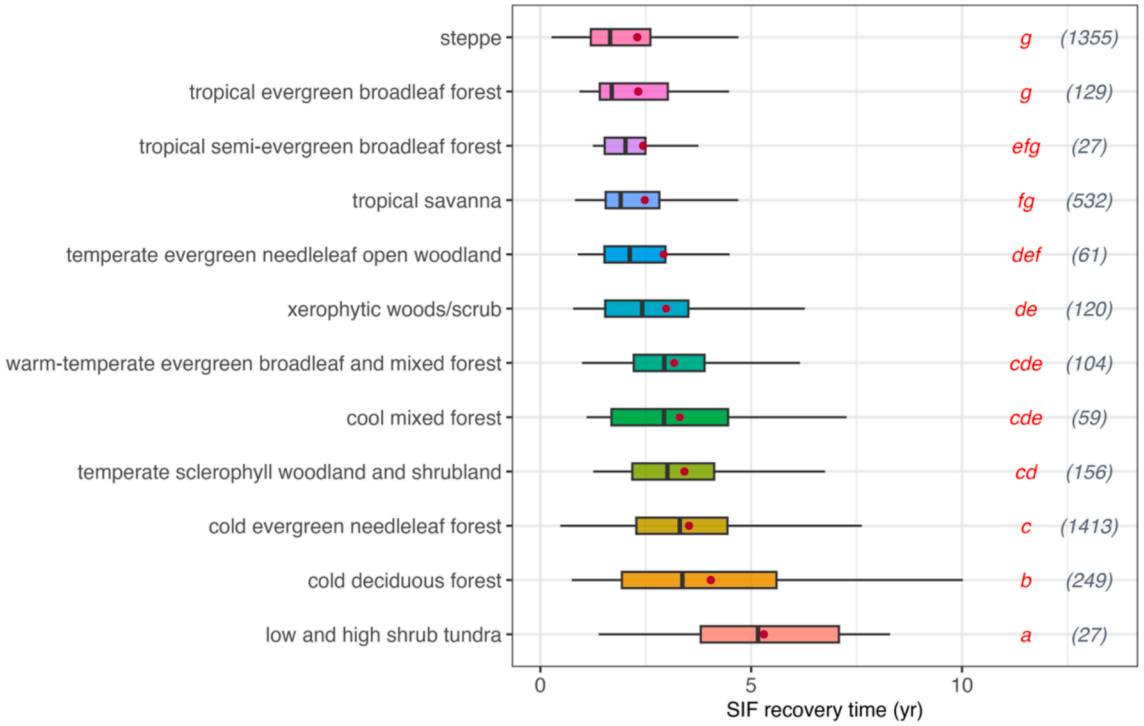

Fig. 4. Post-fire photosynthetic recovery times across biomes after controlling for other factors influencing recovery time. The number of fire candidates in each biome is shown in brackets. Significant differences between biomes, as measured by the *t*-test, are indicated by the red letters.

Table 3
Comparison of model performance for 4232 fire candidates with the dominant biome covers > 50 % of the fire area. Residual Standard Error (RSE) is the estimated standard error of the residuals, AIC is the Akaike's Information Criterion, BIC is the Bayesian Information Criterion, Loglik is the log-likelihood. The adjusted R^2 statistic takes account of the degrees of freedom.

	R^2	adjR^2	RSE	loglik	AIC	BIC
Original model	0.39	0.39	0.57	−3608.00	7242.00	7325.00
Model including biomes	0.43	0.43	0.55	−3454.00	6955.00	7107.00

characteristic of cold climates (e.g., cold evergreen needleleaf forest, tundra), although the differences between biomes in each of these groups is not always significant. Given that the original model already included GPP as a measure of ecosystem characteristics, this analysis suggests that there may be other properties such as adaptations to different fire regimes that influence post-fire recovery time.

3.4. *Fire adaptations as a potential factor influencing recovery time*

We use resprouting as an example of the impact of fire adaptations on post-fire recovery time. The proportion of resprouting species showed a significant variation across biomes: resprouters are more abundant in hot and relatively dry biomes subject to frequent fires, such as xerophytic woods and savannas, and least abundant in biomes characteristic of cold climates, such as tundra (Fig. 5). This is reflected in the relationship with post-fire recovery time: recovery was faster in biomes with a higher abundance of resprouters and slower in biomes where resprouters are rarer (Fig. 5).

4. Discussion

We have shown that recovery time is influenced by vegetation characteristics, fire properties and post-fire climate. GPP appears as the most important factor, with recovery being faster in more productive ecosystems. Measures of ecosystem productivity such as GPP and net primary productivity (NPP) have been used to document the trajectory of post-fire recovery (Amiro et al., 2000; Goulden et al., 2011; Hicke et al., 2003; Xu et al., 2024) but the relationship with long-term productivity levels has not been quantified at a global scale. However, it seems intuitively plausible that more productive ecosystems occur in environments that are favourable for plant growth and therefore will respond to disturbances, including fire, more quickly. This is consistent with a review focusing on forests in Canada, which showed that the recovery time following both wildfire and timber harvest was related to the inherent productivity of the site (Bartels et al., 2016). However, the fact that recovery is also fast in arid ecosystems, as indicated by the importance of dry day length, seems to contradict this general relationship. This may reflect the fact that these ecosystems are characterised by herbaceous plants or shrubs that regrow more quickly than trees, as shown by the fact that that grass cover is higher in regions with a longer dry period (Fig. S2). It could also be because ecosystems that have long dry seasons during which the fuel load becomes dry enough to burn, such as savannas, typically have fires on a regular basis (Keeley and Pausas, 2022) and are therefore likely to be characterised by fire-adapted plants (Simpson et al., 2022), as suggested by the fact that the proportion of resprouters is higher in regions with longer dry periods (Fig. S3), and that the proportion of resprouters influences the speed of recovery. The negative relationship between dry day length and recovery time could also be explained by the adaptation of maximum carboxylation rate to dry climate and the trade-off that exists between photosynthesis and water-use efficiency (Prentice et al., 2014): drier areas have higher photosynthetic efficiency, which means chlorophyll fluorescence will recover faster.

Fire properties also play an important role in determining the vegetation recovery rate. Fires that cause substantial damage to the vegetation increased recovery time. This is consistent with previous studies that have shown that more severe fires lead to longer recovery

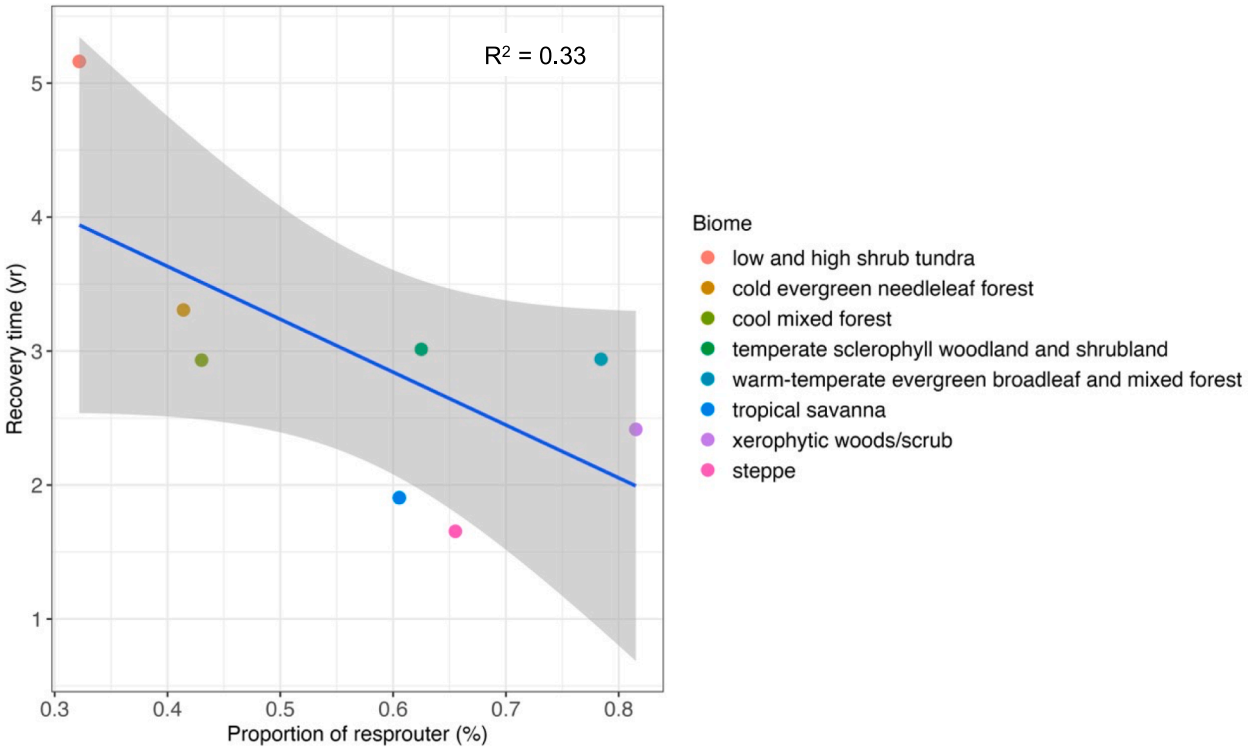

Fig. 5. Relationships between recovery time and proportion of resprouters across biomes using the median of recovery time and proportion of resprouters of each biome.

time (e.g., González-De Vega et al., 2016; Liu, 2016) and also consistent with a global-scale study showing greater combustion-induced vegetation loss causes longer recovery time (Xu et al., 2024). However, some studies focusing on specific forest types, specifically mixed pine-oak forest or coniferous forest, have shown that recovery is faster after high severity fires (e.g., Bright et al., 2019; Meng et al., 2018).The accelerated recovery is attributed to fire adaptations; for example, the dominant pine in mixed pine-oak forest has thick bark and can recover though crown regrowth or epicormic resprouting, while the oaks can produce vigorous sprouts from the root collars. These regional studies, however, did not control for other factors that might influence recovery rate. We have shown that post-fire climate, for example, influences the rate of ecosystem recovery. This is consistent with previous studies that showed that higher than normal precipitation or less than normal dry days both accelerate recovery (Meng et al., 2015; Viana-Soto et al., 2020).

Topographic factors, such as elevation, slope and aspect, do not emerge as important in our analyses. However, topographic factors have been shown to be significant in regional studies. Shryock et al. (2015) and Qiu et al. (2021) found that elevation is one of the strongest predictors of vegetation recovery. Additionally, some northern hemisphere studies, for example, have shown that south-facing slopes are more prone to drought and this results in slower recovery after fire compared to north-facing slopes (Ireland and Petropoulos, 2015; Meng et al., 2015; Mitchell and Yuan, 2010; Viana-Soto et al., 2020; Wittenberg et al., 2007). The lack of importance of topographic factors in our analysis may reflect the fact that this micro-climate control is already accounted for by other predictor variables, such as GPP. It could also reflect differences in spatial resolution between these regional or site-scale studies and our global analysis, which was conducted at relatively coarse resolution (0.05°, approximately 5 km).

Human activity was not found to be important in our global analysis, which is consistent with Xu et al. (2024) who found that human intervention only has minor effect on recovery time at the global scale. However, our analyses at the level of individual biomes showed that factors related to human activities were important for post-fire recovery in non-fire-adapted biomes, such as cold evergreen needleleaf forest, but not in fire-adapted biomes, such as tropical savanna and steppe. A similar distinction between fire-adapted and non-fire-adapted biomes has been found in the degree to which human activities such as landscape fragmentation promote fire occurrence (Harrison et al., 2021; Harrison et al., 2024). This suggests that it would be important to make a distinction between fire-adapted and non-fire-adapted biomes in terms of the role of humans both in promoting fires and in promoting post-fire recovery. However, this would require a more robust and quantitative understanding of ecosystem properties that determine resilience to fire.

We have shown that accounting for biome gives additional explanatory power, and suggested that this is because biomes represent fire adaptations. This is borne out by our analysis of the impact of resprouting on post-fire recovery time, based on quantitative information about the proportion of resprouters from plots in Europe and Australia, which showed that the recovery time was faster in biomes with a higher proportion of resprouters. Field studies also show that resprouting trees exhibit significantly faster recovery rates compared to non-resprouting trees (e.g., Casady et al., 2010; Gouveia et al., 2010; Van Leeuwen et al., 2010). However, resprouting is only one part of the syndrome of vegetation adaptations to fire (Harrison et al., 2021). Fire adaptations such as smoke- or heat-induced germination could also promote fast post-fire recovery, while bark thickness is important in reducing the damage from fire and hence ecosystem resilience. Unfortunately, there is less information available about these fire adaptations than about resprouting, and this precludes detailed analysis of their impact on ecosystem recovery.

Our estimates suggest that post-fire recovery of photosynthetic activity is relatively fast: in 75 % of the cases recovery occurred in < 4 years. Intuitively, these recovery times seem very fast. However, this is not due to methodological choices. Doubling the period used to define the pre-fire ecosystem state or considering the entire fire-free period before each recorded fire to determine the pre-fire state resulted in negligible changes to the SIF target, with recovery times differing by ≤ 1 year for 95 % of the fires analyzed (Fig. S5, Fig. S6). Using a 100 % recovery threshold, rather than the generally accepted level of 90 %, again only extended recovery times by $\leq$ 1-year in 75 % of the fires examined (Fig. S7) although post-fire recovery was extended by 10 years for a very small number of fires (0.5 %). The use of the 90 % threshold was useful because it increased the overall sample size substantially (32 %) and also reduced uncertainty associated with the SIF measurements. Extrapolation of recovery trajectories for fire candidates that had not recovered before the end of the sampling period did result in a lengthening of recovery times for cold evergreen needleleaf forest, cold deciduous forest and steppe, but this did not affect the selection or relative importance of predictor variables (Fig. S8) or the impact of biome type on recovery rate (Fig. S9) since most fire candidates had recovered in the sampled period. However, an extension of the period covered by high-quality fire records would be useful to corroborate these findings.

In this study, we used SIF to analyse the recovery process. SIF provides a direct measurement of photosynthetic activity, reducing the bias caused by vegetation structure or heterogeneity in vegetation age compared to traditional "greenness" monitoring techniques (Guo et al., 2020; Tang et al., 2016). However, recovery of photosynthetic activity is not the same as recovery of above-ground biomass. Fan et al. (2023) showed that the recovery of above-ground live biomass carbon lagged photosynthetic activity in boreal forests in Siberia. Although there are global satellite-derived data sets for above-ground biomass, they are either estimates for single years (e.g. GEDI 4: Dubayah et al., 2022); JPL 2020 Global Biomass Dataset: (Xu et al., 2021) or at best cover only seven years (ESA CCI Global Forest Above Ground Biomass v5: (Santoro and Cartus, 2023), too short an interval to capture recovery after individual fires in forested ecosystems. VOD data have been used to estimate biomass and forest structure, but VOD data sets that cover a relatively long time period are at too coarse a resolution to match to individual fires (e.g. VODCA: Moesinger et al. 2020); Global L-band VOD: (Skulovich et al., 2024) or have sufficient spatial resolution but cover a limited time frame (SMOS-IC: Wigneron et al., 2021). Live fuel moisture content (LFMC) could also be used as a measure of ecosystem recovery, but again available data sets (e.g. Globe-LFMC 2.0: Yebra et al., 2024) are based on spatially clustered training data and are difficult to match with individual fire records. Nevertheless, a complete understanding of post-fire ecosystem recovery will require a better characterisation of biomass and structural recovery, and it would be useful to compare the recovery trajectories of photosynthetic activity and other ecosystem properties when data become available at comparable spatial and temporal resolution to the SIF data.

Our findings have implications for process-based fire-enabled vegetation models currently used to predict the environmental consequences of future climate changes (UNEP Rapid Response Assessment, 2022) and for land-surface models that incorporate fire as an explicit disturbance (Li et al., 2024). GPP is an important predictor of the occurrence of fire (Haas et al., 2022), but we have shown that it is also the most important factor determining recovery time. Forkel et al. (2019) have pointed out that many fire models show an emergent relationship between GPP and burnt area that is inconsistent with the observations. Comparison of simulated GPP against flux-tower observations shows that land-surface models often underestimate GPP at site level (Li et al., 2018; Mengoli et al., 2022; Slevin et al., 2015), possibly because they do not take account of plant acclimation to changing climate (Mengoli et al., 2022). This would impact both fire occurrence and post-fire recovery time, with consequences for the simulated carbon cycle. Our analyses also suggest that other ecosystem properties, such as the prevalence of adaptations to fire that could promote faster recovery, are important. Although DGVMs and LSMs incorporate fire as an explicit disturbance, most do not take account of plant adaptations to fire (Hantson et al., 2016; Kloster and

Lasslop, 2017; Lasslop et al., 2019). However, Kelley et al. (2014) incorporated resprouting as a trait in the LPX-Mv1 DGVM, and showed that it resulted in much faster ecosystem recovery. Deriving robust quantitative relationships between specific fire adaptations and post-fire recovery time is challenging due to limited information on these traits, but our analyses suggest that establishing such relationships and incorporating them into models would improve predictions of the carbon cycle.

5. Conclusion

In this study, we used solar-induced chlorophyll fluorescence (SIF) to quantify the recovery of photosynthetic activity following fire on a global scale. We show that vegetation characteristics, fire properties, and post-fire climatic conditions all influence recovery time. Gross primary productivity (GPP) is the most important factor determining the speed of recovery: recovery is faster in ecosystems characterised by higher productivity overall. Fires characterized by greater intensity and duration, which cause extensive vegetation damage, are associated with longer recovery times. Climate in the period after the fire also influences recovery times: anomalously high temperatures, increased temperature seasonality, and a higher frequency of dry days are linked to slower recovery, whereas above-average precipitation accelerates recovery. Recovery times also vary across biomes, most likely reflecting the prevalence of fire-adaptive traits that enhance ecosystem resilience. This study advances our understanding of the factors driving post-fire ecosystem recovery at a global scale and provides information that could be used to improve fire-vegetation interactions in process-based fire-enabled vegetation models.

Funding information

This research received support through Schmidt Sciences, LLC (YS, SPH, ICP). This work is a contribution to the LEMONTREE (Land Ecosystem Models based On New Theory, obseRvations and ExperimEnts) project, and to the Leverhulme Centre for Wildfires, Environment and Society. ICP acknowledges support from the European Research Council (787203 REALM) under the European Union's Horizon 2020 research programme.

CRediT authorship contribution statement

Yicheng Shen: Writing – review & editing, Writing – original draft, Visualization, Validation, Methodology, Investigation, Formal analysis, Data curation, Conceptualization. **I. Colin Prentice:** Writing – review & editing, Supervision, Methodology, Funding acquisition, Conceptualization. **Sandy P. Harrison:** Writing – review & editing, Writing – original draft, Supervision, Methodology, Funding acquisition, Conceptualization.

Declaration of competing interest

The authors declare that they have no known competing financial interests or personal relationships that could have appeared to influence the work reported in this paper.

Acknowledgments

We thank colleagues in the Land Ecosystem Models based On New Theory, obseRvations and ExperimEnts (LEMONTREE) Project and the Leverhulme Centre for Wildfires, Environment and Society for discussions during the development of this work. We also thank Jianing Fang and Pierre Gentine for providing the LCSIF data.

Appendix A. Supplementary data

Supplementary data to this article can be found online at https://doi.org/10.1016/j.ecolind.2025.113206.

Data availability

Data will be made available on request.

References

Amatulli, G., Domisch, S., Tuanmu, M.-N., Parmentier, B., Ranipeta, A., Malczyk, J., Jetz, W., 2018. A suite of global, cross-scale topographic variables for environmental and biodiversity modeling. Sci. Data. 5, 180040. https://doi.org/10.1038/sdata.2018.40.

Amiro, B.D., Chen, J.M., Liu, J., 2000. Net primary productivity following forest fire for Canadian ecoregions. Can. J. for. Res. 30, 939–947. https://doi.org/10.1139/x00-025.

Andela, N., Jones, M.W., 2024. Update of: The Global Fire Atlas of individual fire size, duration, speed and direction. Zenodo. https://doi.org/10.5281/zenodo.11400062.

Andela, N., Morton, D.C., Giglio, L., Paugam, R., Chen, Y., Hantson, S., Van Der Werf, G. R., Anderson, J.T., 2019. The Global Fire Atlas of individual fire size, duration, speed and direction. Earth Syst. Sci. Data. 11, 529–552. https://doi.org/10.5194/ESSD-11-529-2019.

Baker, N.R., 2008. Chlorophyll fluorescence: a probe of photosynthesis in vivo. Annu. Rev. Plant Biol. 59, 89–113. https://doi.org/10.1146/annurev.arplant.59.032607.092759.

Bartels, S.F., Chen, H.Y.H., Wulder, M.A., White, J.C., 2016. Trends in post-disturbance recovery rates of Canada's forests following wildfire and harvest. For. Ecol. Manag. 361, 194–207. https://doi.org/10.1016/j.foreco.2015.11.015.

Bastos, A., Gouveia, C.M., Dacamara, C.C., Trigo, R.M., 2011. Modelling post-fire vegetation recovery in Portugal. Biogeosciences. 8, 3593–3607. https://doi.org/10.5194/bg-8-3593-2011.

Bond, W.J., Woodward, F.I., Midgley, G.F., 2005. The global distribution of ecosystems in a world without fire. New Phytol. 165, 525–538. https://doi.org/10.1111/j.1469-8137.2004.01252.x.

Bousquet, E., Mialon, A., Rodriguez-Fernandez, N., Mermoz, S., Kerr, Y., 2022. Monitoring post-fire recovery of various vegetation biomes using multi-wavelength satellite remote sensing. Biogeosciences. 19, 3317–3336. https://doi.org/10.5194/bg-19-3317-2022.

Bright, B.C., Hudak, A.T., Kennedy, R.E., Braaten, J.D., Henareh, K.A., 2019. Examining post-fire vegetation recovery with Landsat time series analysis in three western North American forest types. Fire Ecol. 15, 8. https://doi.org/10.1186/s42408-018-0021-9.

Bruelheide, H., Dengler, J., Jiménez-Alfaro, B., Purschke, O., Hennekens, S.M., Chytrý, M., Pillar, V.D., Jansen, F., Kattge, J., Sandel, B., Aubin, I., Biurrun, I., Field, R., Haider, S., Jandt, U., Lenoir, J., Peet, R.K., Peyre, G., Sabatini, F.M., Schmidt, M., Schrodt, F., Winter, M., Aćić, S., Agrillo, E., Alvarez, M., Ambarlı, D., Angelini, P., Apostolova, I., Arfin Khan, M.A.S., Arnst, E., Attorre, F., Baraloto, C., Beckmann, M., Berg, C., Bergeron, Y., Bergmeier, E., Bjorkman, A.D., Bondareva, V., Borchardt, P., Botta-Dukát, Z., Boyle, B., Breen, A., Brisse, H., Byun, C., Cabido, M.R., Casella, L., Cayuela, L., Černý, T., Chepinoga, V., Csiky, J., Curran, M., Ćušterevska, R., Dajić, S.Z., De Bie, E., De Ruffray, P., De Sanctis, M., Dimopoulos, P., Dressler, S., Ejrnæs, R., El-Sheikh, M.A.E.R.M., Enquist, B., Ewald, J., Fagúndez, J., Finckh, M., Font, X., Forey, E., Fotiadis, G., García-Mijangos, I., Gasper, A.L., Golub, V., Gutierrez, A.G., Hatim, M.Z., He, T., Higuchi, P., Holubová, D., Hölzel, N., Homeier, J., Indreica, A., Işık, G.D., Jansen, S., Janssen, J., Jedrzejek, B., Jiroušek, M., Jürgens, N., Kącki, Z., Kavgacı, A., Kearsley, E., Kessler, M., Knollová, I., Kolomiychuk, V., Korolyuk, A., Kozhevnikova, M., Kozub, Ł., Krstonošić, D., Kühl, H., Kühn, I., Kuzemko, A., Küzmič, F., Landucci, F., Lee, M.T., Levesley, A., Li, C.F., Liu, H., Lopez-Gonzalez, G., Lysenko, T., Macanović, A., Mahdavi, P., Manning, P., Marcenò, C., Martynenko, V., Mencuccini, M., Minden, V., Moeslund, J.E., Moretti, M., Müller, J.V., Munzinger, J., Niinemets, Ü., Nobis, M., Noroozi, J., Nowak, A., Onyshchenko, V., Overbeck, G.E., Ozinga, W.A., Pauchard, A., Pedashenko, H., Peñuelas, J., Pérez-Haase, A., Peterka, T., Petřík, P., Phillips, O.L., Prokhorov, V., Rašomavičius, V., Revermann, R., Rodwell, J., Ruprecht, E., Rūsiņa, S., Samimi, C., Schaminée, J.H.J., Schmiedel, U., Šibík, J., Šilc, U., Škvorc, Ž., Smyth, A., Sop, T., Sopotlieva, D., Sparrow, B., Stančić, Z., Svenning, J.C., Swacha, G., Tang, Z., Tsiripidis, I., Turtureanu, P.D., Uğurlu, E., Uogintas, D., Valachovič, M., Vanselow, K.A., Vashenyak, Y., Vassilev, K., Vélez-Martin, E., Venanzoni, R., Vibrans, A.C., Violle, C., Virtanen, R., Wehrden, H., Wagner, V., Walker, D.A., Wana, D., Weiher, E., Wesche, K., Whitfeld, T., Willner, W., Wiser, S., Wohlgemuth, T., Yamalov, S., Zizka, G., Zverev, A., 2019. sPlot – A new tool for global vegetation analyses. J. Veg. Sci. 30, 161–186. https://doi.org/10.1111/jvs.12710.

Casady, G.M., Van Leeuwen, W.J.D., Marsh, S.E., 2010. Evaluating post-wildfire vegetation regeneration as a response to multiple environmental determinants. Environ Model Assess. 15, 295–307. https://doi.org/10.1007/s10666-009-9210-x.

CIESIN, 2018. Gridded Population of the World, Version 4 (GPWv4): Population Density Adjusted to Match 2015 Revision UN WPP Country Totals, Revision 11 . Center for International Earth Science Information Network (CIESIN), Columbia University, NASA Socioeconomic Data and Applications Center (SEDAC). https://doi.org/10.7927/H49C6VHW.

Clarke, P.J., Lawes, M.J., Midgley, J.J., 2010. Resprouting as a key functional trait in woody plants – challenges to developing new organizing principles. New Phytol. 188, 651–654. https://doi.org/10.1111/j.1469-8137.2010.03508.x.
Clarke, P.J., Lawes, M.J., Midgley, J.J., Lamont, B.B., Ojeda, F., Burrows, G.E., Enright, N.J., Knox, K.J.E., 2013. Resprouting as a key functional trait: how buds, protection and resources drive persistence after fire. New Phytol. 197, 19–35. https://doi.org/10.1111/nph.12001.
De Luca, G., Silva, J.M.N., Modica, G., 2022. Short-term temporal and spatial analysis for post-fire vegetation regrowth characterization and mapping in a Mediterranean ecosystem using optical and SAR image time-series. Geocarto International. 37, 15428–15462. https://doi.org/10.1080/10106049.2022.2097482.
Díaz-Delgado, R., Lloret, F., Pons, X., 2003. Influence of fire severity on plant regeneration by means of remote sensing imagery. Int. J. Remote Sens. 24, 1751–1763. https://doi.org/10.1080/01431160210144732.
Dubayah R.O., Armston J., Kellner J.R., Duncanson L., Healey S.P., Patterson P.L., Hancock S., Tang H., Bruening J., Hofton M.A., Blair J.B., Luthcke S.B., 2022. GEDI L4A Footprint Level Aboveground Biomass Density, Version 2.1. ORNL Distributed Active Archive Center. 10.3334/ORNLDAAC/2056.
Fan, L., Wigneron, J.-P., Ciais, P., Chave, J., Brandt, M., Sitch, S., Yue, C., Bastos, A., Li, X., Qin, Y., Yuan, W., Schepaschenko, D., Mukhortova, L., Li, X., Liu, X., Wang, M., Frappart, F., Xiao, X., Chen, J., Ma, M., Wen, J., Chen, X., Yang, H., Van Wees, D., Fensholt, R., 2023. Siberian carbon sink reduced by forest disturbances. Nat. Geosci. 16, 56–62. https://doi.org/10.1038/s41561-022-01087-x.
Fang J., Liana X., Ryub Y., Jeongb S., Jiange C., Gentinea P., 2023. Reconstruction of a long-term spatially contiguous solar-induced fluorescence (LCSIF) over 1982-2021. arxiv. https://doi.org/10.48550/arXiv.2311.14987.
Forkel, M., Andela, N., Harrison, S.P., Lasslop, G., Van Marle, M., Chuvieco, E., Dorigo, W., Forrest, M., Hantson, S., Heil, A., Li, F., Melton, J., Sitch, S., Yue, C., Arneth, A., 2019. Emergent relationships with respect to burned area in global satellite observations and fire-enabled vegetation models. Biogeosciences. 16, 57–76. https://doi.org/10.5194/bg-16-57-2019.
Francos, M., Úbeda, X., Tort, J., Panareda, J.M., Cerdà, A., 2016. The role of forest fire severity on vegetation recovery after 18 years. Implications for forest management of Quercus suber L. in Iberian Peninsula. Glob. Planet. Change. 145, 11–16. https://doi.org/10.1016/j.gloplacha.2016.07.016.
Giglio, L., Csiszar, I., Justice, C.O., 2006. Global distribution and seasonality of active fires as observed with the Terra and Aqua Moderate Resolution Imaging Spectroradiometer (MODIS) sensors. Journal of Geophysical Research: Biogeosciences. 111, G02016. https://doi.org/10.1029/2005JG000142.
Giorgis, M.A., Zeballos, S.R., Carbone, L., Zimmermann, H., von Wehrden, H., Aguilar, R., Ferreras, A.E., Tecco, P.A., Kowaljow, E., Barri, F., Gurvich, D.E., Villagra, P., Jaureguiberry, P., 2021. A review of fire effects across South American ecosystems: the role of climate and time since fire. Fire Ecol. 17. https://doi.org/10.1186/s42408-021-00100-9.
Gitas, I., Mitri, G., Veraverbeke, S., Polychronaki, A., 2012. Advances in remote sensing of post-fire vegetation recovery monitoring—a review. Remote Sensing of Biomass-Principles and Applications. 1, 334. https://doi.org/10.5772/20571.
González-De Vega S., De las Heras J., Moya D., 2016. Resilience of Mediterranean terrestrial ecosystems and fire severity in semiarid areas: Responses of Aleppo pine forests in the short, mid and long term. Sci. Total Environ. 573, 1171-1177. https://doi.org/10.1016/j.scitotenv.2016.03.115.
Goulden, M.L., Mcmillan, A.M.S., Winston, G.C., Rocha, A.V., Manies, K.L., Harden, J.W., Bond-Lamberty, B.P., 2011. Patterns of NPP, GPP, respiration, and NEP during boreal forest succession. Glob. Change Biol. 17, 855–871. https://doi.org/10.1111/j.1365-2486.2010.02274.x.
Gouveia, C., Dacamara, C.C., Trigo, R.M., 2010. Post-fire vegetation recovery in Portugal based on spot/vegetation data. Nat. Hazards Earth Syst. Sci. 10, 673–684. https://doi.org/10.5194/nhess-10-673-2010.
Guo, M., Li, J., Huang, S., Wen, L., 2020. Feasibility of using MODIS products to simulate Sun-Induced Chlorophyll Fluorescence (SIF) in boreal forests. Remote Sens. 12, 680. https://doi.org/10.3390/rs12040680.
Guo, M., Li, J., Yu, F., Yin, S., Huang, S., Wen, L., 2021. Estimation of post-fire vegetation recovery in boreal forests using solar-induced chlorophyll fluorescence (SIF) data. Int. J. Wildland Fire. 30, 365–377. https://doi.org/10.1071/WF20162.
Haas, O., Prentice, I.C., Harrison, S.P., 2022. Global environmental controls on wildfire burnt area, size, and intensity. Environ. Res. Lett. 17, 065004. https://doi.org/10.1088/1748-9326/ac6a69.
Hantson, S., Arneth, A., Harrison, S.P., Kelley, D.I., Prentice, I.C., Rabin, S.S., Archibald, S., Mouillot, F., Arnold, S.R., Artaxo, P., Bachelet, D., Ciais, P., Forrest, M., Friedlingstein, P., Hickler, T., Kaplan, J.O., Kloster, S., Knorr, W., Lasslop, G., Li, F., Mangeon, S., Melton, J.R., Meyn, A., Sitch, S., Spessa, A., Van Der Werf, G.R., Voulgarakis, A., Yue, C., 2016. The status and challenge of global fire modelling. Biogeosciences. 13, 3359–3375. https://doi.org/10.5194/bg-13-3359-2016.
Harper, K.L., Lamarche, C., Hartley, A., Peylin, P., Ottlé, C., Bastrikov, V., San, M.R., Bohnenstengel, S.I., Kirches, G., Boettcher, M., Shevchuk, R., Brockmann, C., Defourny, P., 2023. A 29-year time series of annual 300 m resolution plant-functional-type maps for climate models. Earth Syst. Sci. Data. 15, 1465–1499. https://doi.org/10.5194/essd-15-1465-2023.
Harrison S.P., Marlon J.R., Bartlein P.J., 2010. Fire in the Earth system, in: Dodson J., (Eds.), Changing Climates, Earth Systems and Society. Springer Netherlands. Dordrecht, pp. 21-48. 10.1007/978-90-481-8716-4_3.
Harrison, S.P., Haas, O., Bartlein, P.J., Sweeney, L., Zhang, G., 2024. (in press). Climate, vegetation, people: disentangling the controls of fire at different timescales. Phil. Trans. 0.1098/rstb.2023-0464.
Harrison, S.P., Prentice, I.C., Bloomfield, K.J., Dong, N., Forkel, M., Forrest, M., Ningthoujam, R.K., Pellegrini, A., Shen, Y., Baudena, M., Cardoso, A.W., Huss, J.C., Joshi, J., Oliveras, I., Pausas, J.G., Simpson, K.J., 2021. Understanding and modelling wildfire regimes: an ecological perspective. Environ. Res. Lett. 16, 125008. https://doi.org/10.1088/1748-9326/ac39be.
Hastie, T., Tibshirani, R., Tibshirani, R., 2020. Best subset, forward stepwise or lasso? Analysis and recommendations based on extensive comparisons. Stat. Sci. 35 (579–592), 14. https://doi.org/10.1214/19-STS733.
Hengl, T., 2018. Potential distribution of biomes (Potential Natural Vegetation) at 250 m spatial resolution. Zenodo. https://doi.org/10.5281/zenodo.10513520.
Hengl, T., Walsh, M.G., Sanderman, J., Wheeler, I., Harrison, S.P., Prentice, I.C., 2018. Global mapping of potential natural vegetation: an assessment of machine learning algorithms for estimating land potential. PeerJ. 6, e5457.
Hersbach H., Bell B., Berrisford P., Biavati G., Horányi A., Muñoz Sabater J., Nicolas J., Peubey C., Radu R., Rozum I., Schepers D., Simmons A., Soci C., Dee D., Thépaut J.-N., 2023. ERA5 hourly data on single levels from 1940 to present . Copernicus Climate Change Service (C3S) Climate Data Store (CDS). 10.24381/cds.adbb2d47.
Hicke, J.A., Asner, G.P., Kasischke, E.S., French, N.H.F., Randerson, J.T., Collatz, G.J., Stocks, B.J., Tucker, C.J., Los, S.O., Field, C.B., 2003. Postfire response of North American boreal forest net primary productivity analyzed with satellite observations. Glob. Change Biol. 9, 1145–1157. https://doi.org/10.1046/j.1365-2486.2003.00658.x.
Ireland, G., Petropoulos, G.P., 2015. Exploring the relationships between post-fire vegetation regeneration dynamics, topography and burn severity: a case study from the Montane Cordillera Ecozones of Western Canada. Appl. Geogr. 56, 232–248. https://doi.org/10.1016/j.apgeog.2014.11.016.
Irteza, S.M., Nichol, J.E., Shi, W., Abbas, S., 2021. NDVI and fluorescence indicators of seasonal and structural changes in a tropical forest succession. Earth Syst. Environ. 5, 127–133. https://doi.org/10.1007/s41748-020-00175-5.
Jennings, M.D., Harris, G.M., 2017. Climate change and ecosystem composition across large landscapes. Landsc. Ecol. 32, 195–207. https://doi.org/10.1007/s10980-016-0435-1.
Jeong, S., Ryu, Y., Gentine, P., Lian, X., Fang, J., Li, X., Dechant, B., Kong, J., Choi, W., Jiang, C., Keenan, T.F., Harrison, S.P., Prentice, I.C., 2024. Persistent global greening over the last four decades using novel long-term vegetation index data with enhanced temporal consistency. Remote Sens. Environ. 311, 114282. https://doi.org/10.1016/j.rse.2024.114282.
João, T., João, G., Bruno, M., João, H., 2018. Indicator-based assessment of post-fire recovery dynamics using satellite NDVI time-series. Ecol. Indic. 89, 199–212. https://doi.org/10.1016/j.ecolind.2018.02.008.
Jucker, R.M., Liniger, H., Valdecantos, A., Schwilch, G., 2016. Impacts of land management on the resilience of Mediterranean dry forests to fire. Sustainability. 8, 981. https://doi.org/10.3390/su8100981.
Keeley, J.E., 2009. Fire intensity, fire severity and burn severity: a brief review and suggested usage. Int. J. Wildland Fire. 18, 116–126. https://doi.org/10.1071/WF07049.
Keeley, J.E., Pausas, J.G., 2022. Evolutionary ecology of fire. Annu. Rev. Ecol. Evol. Syst. 53, 203–225. https://doi.org/10.1146/annurev-ecolsys-102320-095612.
Kelley, D.I., Harrison, S.P., Prentice, I.C., 2014. Improved simulation of fire-vegetation interactions in the Land surface Processes and eXchanges dynamic global vegetation model (LPX-Mv1). Geosci. Model Dev. 7, 2411–2433. https://doi.org/10.5194/gmd-7-2411-2014.
Kloster, S., Lasslop, G., 2017. Historical and future fire occurrence (1850 to 2100) simulated in CMIP5 Earth System Models. Glob. Planet. Change. 150, 58–69. https://doi.org/10.1016/j.gloplacha.2016.12.017.
Kruger F.J., 1984. Effects of Fire on Vegetation Structure and Dynamics, in: Booysen P.V. d., Tainton N.M., (Eds.), Ecological Studies. Springer. Berlin, pp. 219-243. https://doi.org/10.1007/978-3-642-69805-7_10.
Lasslop, G., Coppola, A.I., Voulgarakis, A., Yue, C., Veraverbeke, S., 2019. Influence of fire on the carbon cycle and climate. Curr. Clim. Change Rep. 5, 112–123. https://doi.org/10.1007/s40641-019-00128-9.
Lawes, M.J., Clarke, P.J., 2011. Ecology of plant resprouting: populations to community responses in fire-prone ecosystems. Plant Ecol. 212, 1937–1943. https://doi.org/10.1007/s11258-011-9994-z.
Li, B., Ryu, Y., Jiang, C., Dechant, B., Liu, J., Yan, Y., Li, X., 2023. BESSv2.0: a satellite-based and coupled-process model for quantifying long-term global land–atmosphere fluxes. Remote Sens. Environ. 295, 113696. https://doi.org/10.1016/j.rse.2023.113696.
Li, F., Lawrence, D.M., 2017. Role of fire in the global land water budget during the twentieth century due to changing ecosystems. J. Climate. 30, 1893–1908. https://doi.org/10.1175/jcli-d-16-0460.1.
Li F., Song X., Harrison S.P., Marlon J.R., Lin Z., Leung L.R., Schwinger J., Marécal V., Wang S., Ward D.S., Dong X., Lee H., Nieradzik L., Rabin S.S., Séférian R., 2024. Evaluation of global fire simulations in CMIP6 Earth system models [preprint]. Geosci. Model Dev. 10.5194/gmd-2024-85.
Li, J., Duan, Q., Wang, Y.P., Gong, W., Gan, Y., Wang, C., 2018. Parameter optimization for carbon and water fluxes in two global land surface models based on surrogate modelling. Int. J. Climatol. 38, e1016–e1031. https://doi.org/10.1002/joc.5428.
Liu, F., Qin, Q., Zhan, Z., 2012. A novel dynamic stretching solution to eliminate saturation effect in NDVI and its application in drought monitoring China. Geogr. Sci. 22, 683–694. https://doi.org/10.1007/s11769-012-0574-5.
Liu, Z., 2016. Effects of climate and fire on short-term vegetation recovery in the boreal larch forests of Northeastern China. Sci. Rep. 6, 37572. https://doi.org/10.1038/srep37572.
Marcos, B., Gonçalves, J., Alcaraz-Segura, D., Cunha, M., Honrado, J.P., 2023. Assessing the resilience of ecosystem functioning to wildfires using satellite-derived metrics of

post-fire trajectories. Remote Sens. Environ. 286, 113441. https://doi.org/10.1016/j.rse.2022.113441.
Meinshausen, N., 2007. Relaxed Lasso. Comput. Stat. Data Anal. 52, 374–393. https://doi.org/10.1016/j.csda.2006.12.019.
Meng, R., Dennison, P.E., Huang, C., Moritz, M.A., D'Antonio, C., 2015. Effects of fire severity and post-fire climate on short-term vegetation recovery of mixed-conifer and red fir forests in the Sierra Nevada Mountains of California. Remote Sens. Environ. 171, 311–325. https://doi.org/10.1016/j.rse.2015.10.024.
Meng, R., Wu, J., Zhao, F., Cook, B.D., Hanavan, R.P., Serbin, S.P., 2018. Measuring short-term post-fire forest recovery across a burn severity gradient in a mixed pine-oak forest using multi-sensor remote sensing techniques. Remote Sens. Environ. 210, 282–296. https://doi.org/10.1016/j.rse.2018.03.019.
Mengoli, G., Agustí-Panareda, A., Boussetta, S., Harrison, S.P., Trotta, C., Prentice, I.C., 2022. Ecosystem photosynthesis in land-surface models: a first-principles approach incorporating acclimation. J. Adv. Model. Earth Syst. 14. https://doi.org/10.1029/2021ms002767.
Meroni, M., Rossini, M., Guanter, L., Alonso, L., Rascher, U., Colombo, R., Moreno, J., 2009. Remote sensing of solar-induced chlorophyll fluorescence: review of methods and applications. Remote Sens. Environ. 113, 2037–2051. https://doi.org/10.1016/j.rse.2009.05.003.
Mitchell, M., Yuan, F., 2010. Assessing forest fire and vegetation recovery in the Black Hills South Dakota. Gisci. Remote Sens. 47, 276–299. https://doi.org/10.2747/1548-1603.47.2.276.
Moesinger, L., Dorigo, W., De Jeu, R., Van Der Schalie, R., Scanlon, T., Teubner, I., Forkel, M., 2020. The global long-term microwave vegetation optical depth climate archive (VODCA). Earth Syst. Sci. Data. 12, 177–196. https://doi.org/10.5194/essd-12-177-2020.
Mohammed, G.H., Colombo, R., Middleton, E.M., Rascher, U., van der Tol, C., Nedbal, L., Goulas, Y., Pérez-Priego, O., Damm, A., Meroni, M., Joiner, J., Cogliati, S., Verhoef, W., Malenovský, Z., Gastellu-Etchegorry, J.-P., Miller, J.R., Guanter, L., Moreno, J., Moya, I., Berry, J.A., Frankenberg, C., Zarco-Tejada, P.J., 2019. Remote sensing of solar-induced chlorophyll fluorescence (SIF) in vegetation: 50years of progress. Remote Sens. Environ. 231, 111177. https://doi.org/10.1016/j.rse.2019.04.030.
Pausas, J.G., Keeley, J.E., 2009. A burning story: the role of fire in the history of life. Bioscience. 59, 593–601. https://doi.org/10.1525/bio.2009.59.7.10.
Prentice, I.C., Dong, N., Gleason, S.M., Maire, V., Wright, I.J., 2014. Balancing the costs of carbon gain and water transport: testing a new theoretical framework for plant functional ecology. Ecol. Lett. 17, 82–91. https://doi.org/10.1111/ele.12211.
Qin, Y., Xiao, X., Wigneron, J.-P., Ciais, P., Canadell, J.G., Brandt, M., Li, X., Fan, L., Wu, X., Tang, H., Dubayah, R., Doughty, R., Crowell, S., Zheng, B., Moore, B., 2022. Large loss and rapid recovery of vegetation cover and aboveground biomass over forest areas in Australia during 2019–2020. Remote Sens. Environ. 278, 113087. https://doi.org/10.1016/j.rse.2022.113087.
Qiu, J., Wang, H., Shen, W., Zhang, Y., Su, H., Li, M., 2021. Quantifying forest fire and post-fire vegetation recovery in the Daxin'anling area of northeastern China using Landsat time-series data and machine learning. Remote Sens. 13, 792. https://doi.org/10.3390/rs13040792.
Sabatini, F.M., Lenoir, J., Hattab, T., Arnst, E.A., Chytrý, M., Dengler, J., De Ruffray, P., Hennekens, S.M., Jandt, U., Jansen, F., Jiménez-Alfaro, B., Kattge, J., Levesley, A., Pillar, V.D., Purschke, O., Sandel, B., Sultana, F., Aavik, T., Aćić, S., Acosta, A.T.R., Agrillo, E., Alvarez, M., Apostolova, I., Arfin Khan, M.A.S., Arroyo, L., Attorre, F., Aubin, I., Banerjee, A., Bauters, M., Bergeron, Y., Bergmeier, E., Biurrun, I., Bjorkman, A.D., Bonari, G., Bondareva, V., Brunet, J., Čarni, A., Casella, L., Cayuela, L., Černý, T., Chepinoga, V., Csiky, J., Ćušterevska, R., De Bie, E., Gasper, A. L., De Sanctis, M., Dimopoulos, P., Dolezal, J., Dziuba, T., El-Sheikh, M.A.E.R.M., Enquist, B., Ewald, J., Fazayeli, F., Field, R., Finckh, M., Gachet, S., Galán-De-Mera, A., Garbolino, E., Gholizadeh, H., Giorgis, M., Golub, V., Alsos, I.G., Grytnes, J. A., Guerin, G.R., Gutiérrez, A.G., Haider, S., Hatim, M.Z., Hérault, B., Hinojos, M.G., Hölzel, N., Homeier, J., Hubau, W., Indreica, A., Janssen, J.A.M., Jedrzejek, B., Jentsch, A., Jürgens, N., Kącki, Z., Kapfer, J., Karger, D.N., Kavgacı, A., Kearsley, E., Kessler, M., Khanina, L., Killeen, T., Korolyuk, A., Kreft, H., Kühl, H.S., Kuzemko, A., Landucci, F., Lengyel, A., Lens, F., Lingner, D.V., Liu, H., Lysenko, T., Mahecha, M. D., Marcenò, C., Martynenko, V., Moeslund, J.E., Monteagudo, M.A., Mucina, L., Müller, J.V., Munzinger, J., Naqinezhad, A., Noroozi, J., Nowak, A., Onyshchenko, V., Overbeck, G.E., Pärtel, M., Pauchard, A., Peet, R.K., Peñuelas, J., Pérez-Haase, A., Peterka, T., Petřík, P., Peyre, G., Phillips, O.L., Prokhorov, V., Rašomavičius, V., Revermann, R., Rivas-Torres, G., Rodwell, J.S., Ruprecht, E., Rūsiņa, S., Samimi, C., Schmidt, M., Schrodt, F., Shan, H., Shirokikh, P., Šibík, J., Šilc, U., Sklenář, P., Škvorc, Ž., Sparrow, B., Sperandii, M.G., Stančić, Z., Svenning, J. C., Tang, Z., Tang, C.Q., Tsiripidis, I., Vanselow, K.A., Vásquez, M.R., Vassilev, K., Vélez-Martin, E., Venanzoni, R., Vibrans, A.C., Violle, C., Virtanen, R., Wehrden, H., Wagner, V., Walker, D.A., Waller, D.M., Wang, H.F., Wesche, K., Whitfeld, T.J.S., Willner, W., Wiser, S.K., Wohlgemuth, T., Yamalov, S., Zobel, M., Bruelheide, H., Bates, A., 2021. sPlotOpen – an environmentally balanced, open-access, global dataset of vegetation plots. Glob. Ecol. Biogeogr. 30, 1740–1764. https://doi.org/10.1111/geb.13346.
Santoro, M., Cartus, O., 2023. ESA Biomass Climate Change Initiative (Biomass_cci): Global datasets of forest above-ground biomass for the years 2010, 2017, 2018, 2019 and 2020. CEDA Archive. https://doi.org/10.5285/af60720c1e404a9e9d2c145d2b2ead4e.
Sato L.Y., Faria Gomes V.C., Shimabukuro Y.E., Keller M., Arai E., Nara dos-Santos M., Brown I.F., Oliveira e Cruz de Aragao L.E., 2016. Post-fire changes in forest biomass retrieved by airborne LiDAR in Amazonia. Remote Sens. 8, 839. 10.3390/rs8100839.
Shen, Y., Cai, W., Prentice, I.C., Harrison, S.P., 2023. Community abundance of resprouting in woody plants reflects fire return time, intensity, and type. Forests. 14, 878. https://doi.org/10.3390/f14050878.
Shryock, D.F., Esque, T.C., Chen, F.C., 2015. Topography and climate are more important drivers of long-term, post-fire vegetation assembly than time-since-fire in the Sonoran Desert US. J. Veg. Sci. 26, 1134–1147. https://doi.org/10.1111/jvs.12324.
Simpson, K.J., Archibald, S., Osborne, C.P., 2022. Savanna fire regimes depend on grass trait diversity. Trends Ecol. Evol. 37, 749–758. https://doi.org/10.1016/j.tree.2022.04.010.
Skulovich, O., Li, X., Wigneron, J.-P., Gentine, P., 2024. Global L-band equivalent AI-based vegetation optical depth dataset. Sci. Data. 11, 936. https://doi.org/10.1038/s41597-024-03810-2.
Slevin, D., Tett, S.F.B., Williams, M., 2015. Multi-site evaluation of the JULES land surface model using global and local data. Geosci. Model Dev. 8, 295–316. https://doi.org/10.5194/gmd-8-295-2015.
Smit, I.P.J., Asner, G.P., Govender, N., Kennedy-Bowdoin, T., Knapp, D.E., Jacobson, J., 2010. Effects of fire on woody vegetation structure in African savanna. Ecol. Appl. 20, 1865–1875. https://doi.org/10.1890/09-0929.1.
Tang, J., Körner, C., Muraoka, H., Piao, S., Shen, M., Thackeray, S.J., Yang, X., 2016. Emerging opportunities and challenges in phenology: a review. Ecosphere. 7, e01436. https://doi.org/10.1002/ecs2.1436.
Tay, J.K., Narasimhan, B., Hastie, T., 2023. Elastic net regularization paths for all generalized linear models. J. Stat. Softw. 106, 10.18637/jss.v106.i01.
Turner, M.G., Romme, W.H., Gardner, R.H., Hargrove, W.W., 1997. Effects of fire size and pattern on early succession in Yellowstone National Park. Ecol. Monogr. 67, 411–433. https://doi.org/10.1890/0012-9615(1997)067[0411:EOFSAP]2.0.CO;2.
UNEP. Spreading like wildfire: the rising threat of extraordinary landscape fires, A UNEP Rapid Response Assessment, Nairobi, 2022.
Van Leeuwen, W., Casady, G., Neary, D., Bautista, S., Alloza, J., Carmel, Y., Wittenberg, L., Malkinson, D., Orr, B.J., 2010. Monitoring post-wildfire vegetation response with remotely sensed time-series data in Spain, USA and Israel. Int. J. Wildland Fire. 19, 75–93. https://doi.org/10.1071/WF08078.
Viana-Soto, A., Aguado, I., Martínez, S., 2017. Assessment of post-fire vegetation recovery using fire severity and geographical data in the Mediterranean region (Spain). Environments. 4, 90. https://doi.org/10.3390/environments4040090.
Viana-Soto, A., Aguado, I., Salas, J., García, M., 2020. Identifying post-fire recovery trajectories and driving factors using Landsat time series in fire-prone Mediterranean pine forests. Remote Sens. 12, 1499. https://doi.org/10.3390/rs12091499.
Viana-Soto, A., García, M., Aguado, I., Salas, J., 2022. Assessing post-fire forest structure recovery by combining LiDAR data and Landsat time series in Mediterranean pine forests. Int. J. Appl. Earth Obs. Geoinf. 108, 102754. https://doi.org/10.1016/j.jag.2022.102754.
Wang, G., Liu, S., Liu, T., Fu, Z., Yu, J., Xue, B., 2019. Modelling above-ground biomass based on vegetation indexes: a modified approach for biomass estimation in semi-arid grasslands. Int. J. Remote Sens. 40, 3835–3854. https://doi.org/10.1080/01431161.2018.1553319.
Wigneron, J.-P., Li, X., Frappart, F., Fan, L., Al-Yaari, A., De Lannoy, G., Liu, X., Wang, M., Le Masson, E., Moisy, C., 2021. SMOS-IC data record of soil moisture and L-VOD: historical development, applications and perspectives. Remote Sens. Environ. 254, 112238. https://doi.org/10.1016/j.rse.2020.112238.
Wittenberg, L., Malkinson, D., Beeri, O., Halutzy, A., Tesler, N., 2007. Spatial and temporal patterns of vegetation recovery following sequences of forest fires in a Mediterranean landscape Mt. Carmel Israel. CATENA. 71, 76–83. https://doi.org/10.1016/j.catena.2006.10.007.
Xu, H., Chen, H.W., Chen, D., Wang, Y., Yue, X., He, B., Guo, L., Yuan, W., Zhong, Z., Huang, L., Zheng, F., Li, T., He, X., 2024. Global patterns and drivers of post-fire vegetation productivity recovery. Bioscience. https://doi.org/10.1038/s41561-024-01520-3.
Xu L., Saatchi S.S., Yang Y., Yu Y., Pongratz J., Bloom A.A., Bowman K., Worden J., Liu J., Yin Y., Domke G., McRoberts R.E., Woodall C., Nabuurs G.-J., de-Miguel S., Keller M., Harris N., Maxwell S., Schimel D., 2021. Changes in global terrestrial live biomass over the 21st century. Sci. Adv. 7, eabe9829. 10.1126/sciadv.abe9829.
Yebra, M., Scortechini, G., Adeline, K., Aktepe, N., Almoustafa, T., Bar-Massada, A., Beget, M.E., Boer, M., Bradstock, R., Brown, T., Castro, F.X., Chen, R., Chuvieco, E., Danson, M., Değirmenci, C.Ü., Delgado-Dávila, R., Dennison, P., Di Bella, C., Domenech, O., Féret, J.-B., Forsyth, G., Gabriel, E., Gagkas, Z., Gharbi, F., Granda, E., Griebel, A., He, B., Jolly, M., Kotzur, I., Kraaij, T., Kristina, A., Kütküt, P., Limousin, J.-M., Martín, M.P., Monteiro, A.T., Morais, M., Moreira, B., Mouillot, F., Msweli, S., Nolan, R.H., Pellizzaro, G., Qi, Y., Quan, X., Resco De Dios, V., Roberts, D., Tavşanoğlu, Ç., Taylor, A.F.S., Taylor, J., Tüfekcioğlu, İ., Ventura, A., Younes, C.N., 2024. Globe-LFMC 2.0, an enhanced and updated dataset for live fuel moisture content research. Sci. Data. 11. https://doi.org/10.1038/s41597-024-03159-6.
Zhang, Y., Peñuelas, J., 2023. Combining solar-induced chlorophyll fluorescence and optical vegetation indices to better understand plant phenological responses to global change. J. Remote Sens. 3, 0085. https://doi.org/10.34133/remotesensing.0085.
Zhou, Z., Liu, L., Jiang, L., Feng, W., Samsonov, S.V., 2019. Using long-term SAR backscatter data to monitor post-fire vegetation recovery in tundra environment. Remote Sens. 11, 2230. https://doi.org/10.3390/rs11192230.